

Nonlinear thermoelectricity in point-contacts at pinch-off: a catastrophe aids cooling

Robert S. Whitney¹

¹ *Laboratoire de Physique et Modélisation des Milieux Condensés (UMR 5493),
Université Grenoble 1, Maison des Magistères, B.P. 166, 38042 Grenoble, France.*

(Dated: August 30, 2012 — Last revision July 18, 2013)

I consider refrigeration and heat engine circuits based on the nonlinear thermoelectric response of point-contacts at pinch-off, allowing for electrostatic interaction effects. I show that a refrigerator can cool to much lower temperatures than predicted by the thermoelectric figure of merit ZT (which is based on linear-response arguments). The lowest achievable temperature has a discontinuity, called a *fold catastrophe* in mathematics, at a critical driving current $I = I_c$. For $I > I_c$ one can in principle cool to absolute zero, when for $I < I_c$ the lowest temperature is about half the ambient temperature. Heat back-flow due to phonons and photons stop cooling at a temperature above absolute zero, and above a certain threshold turns the discontinuity into a sharp cusp. I also give a heuristic condition for when an arbitrary system's nonlinear response means that its ZT ceases to indicate (even qualitatively) the lowest temperature to which the system can refrigerate.

I. INTRODUCTION

Nanostructures often have thermoelectric responses, with electrical-currents causing heat-currents, and vice-versa^{1–3}. There have recently been a number of proposals for nanostructures or molecules with large thermoelectric responses^{4–11} which could have engineering applications for efficient thermoelectric power-generation and refrigeration. In particular, it is hoped that they could cool electrons well below the temperature of standard cryostats^{12–15}, which are increasingly inefficient at sub-Kelvin temperatures.

However, *good* nanostructure refrigerators (those which cool to significantly below their environment's temperature) are rarely in the linear-response regime. Linear-response theory works for small temperature drops (compared with the average temperature) at the scale of the nanostructure and the scale of the electron's inelastic scattering length. This is often the case in bulk semiconductors^{16,17}, but *not* in such nanostructures. See, for example, experiments on refrigeration with S-N tunnel junctions, that generate a temperature drop from 300mK to 100mK across a tunnel junction^{12–15}.

Unfortunately, there is no general theory for the *non-linear* response of quantum systems, because interaction effects are usually significant, and must be modeled using approximations appropriate for the system in question. Here, I calculate the *fully* nonlinear thermoelectric response of a point-contact at pinch off. This system is one of the main candidates for a nanoscale thermoelectric, and its linear (and nearly linear) thermoelectric response is well-studied experimentally^{18,19} and theoretically^{18,20–22}. I consider this thermoelectric response when the temperature drop across the point-contact is of order the average temperature, for which the response is far outside its linear regime. This can be modeled with a nonlinear Landauer-Büttiker scattering theory^{23–27} for thermoelectric heat-transport²⁸. I find that the dimensionless figure of merit, ZT , ceases to be a good measure of the thermoelectric response out-

side the linear regime. Electricity generation is *worse* than linear-response theory indicates, but refrigeration is *better* (achieving much lower temperatures than linear-response theory predicts). Indeed, the lowest temperature of the refrigerator is a discontinuous function of the electrical current. This discontinuity — a fold catastrophe in mathematical language — occurs at a critical current I_c , and helps refrigeration. For currents $I < I_c$ the refrigerator cannot cool below a finite temperature (about half the ambient temperature for $I \rightarrow I_c$), while for $I > I_c$ it passes the catastrophe and can *in principle* cool to absolute zero (see Fig. 1).

In practice a thermoelectric device's quality is reduced by the nonlinear back-flow of heat carried by chargeless particles; phonons and photons. When such back-flow effects are weak, the catastrophe is little affected, but cooling stops at a temperature above absolute zero. At a critical value of back-flow effects, the catastrophe becomes a cusp (discontinuity in the derivative) of the de-

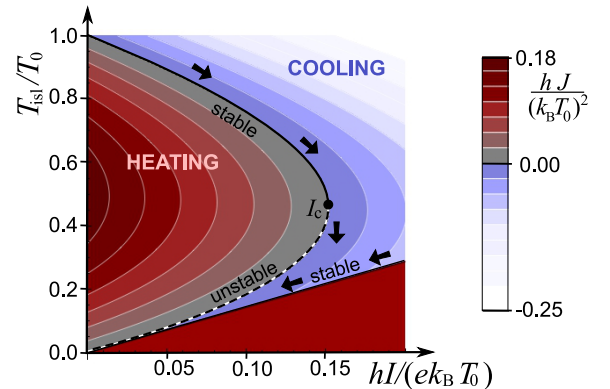


Figure 1: Heat-current $J(T_{isl}, I)$ through a point-contact when driven with a current I , for negligible phonon or photon heating. Blue indicates cooling of the island in Fig. 2a, while red indicates heating. The solid curve is the steady-state ($J = 0$), with the catastrophe at I_c . The straight line is the maximum current, I_{max} , corresponding to infinite bias.

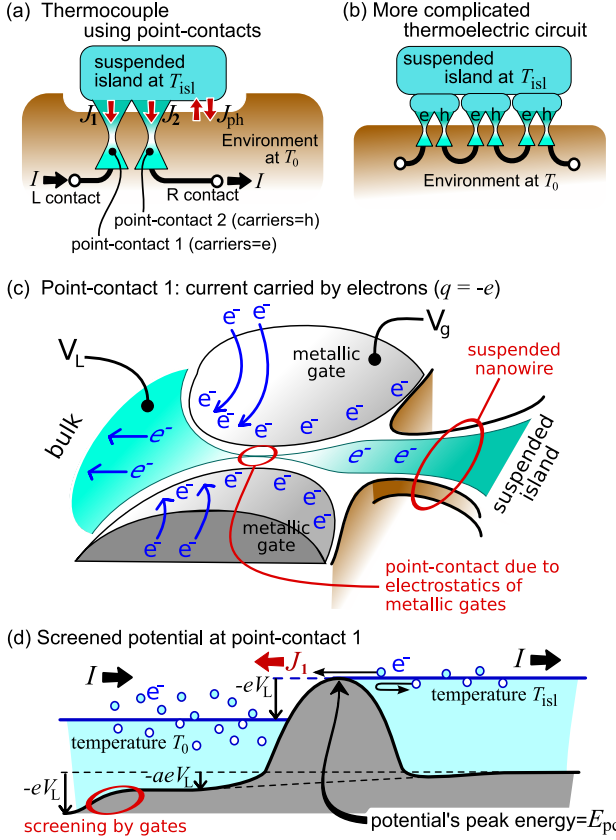


Figure 2: Thermoelectric circuits made with point-contacts shown in (a,b); “e” (“h”) means the point-contact is in a material whose charge-carriers are electrons (holes). One should minimize the heat-current carried by phonons and photons, J_{ph} , by suspending the island^{29,30}. The temperature of the island in similar set-ups (albeit not suspended) has been probed experimentally using a quantum dot as thermometer³¹, although not yet in the regime of refrigeration. (c) Motion of charges in the gates (arrows) caused by making V_L positive, which partially screens V_L at some distance from the point-contact. (d) Point-contact 1 tuned to pinch-off (E_{pc} equals the island’s chemical potential) by adjusting V_g .

pendence of the lowest temperature on I . The nonlinear nature of the cusp still means the lowest achievable temperature is lower than linear theory predicts.

II. NEARLY-LINEAR ANALYSIS FOR ANY SYSTEM, AND ITS BREAKDOWN

The usual “nearly-linear” analysis¹ takes linear response theory plus a Joule heating term, and enables one to quantify devices in terms of their dimensionless figure of merit $ZT = G\Pi^2/((\Theta_{el} + \Theta_{ph})T)$, where T is the device temperature, Π is its Peltier coefficient, G and Θ_{el} are electrical and thermal conductances of electrons, while Θ_{ph} is the thermal conductivity of chargeless excitations, principally phonons and photons. This nearly-linear analysis predicts electric power generation (when

the island is heated) with an efficiency

$$\eta = \frac{\sqrt{ZT+1}-1}{\sqrt{ZT+1}+1} \left(1 - \frac{T_0}{T_{isl}}\right), \quad (1)$$

where T_{isl} and T_0 are the island and environment temperatures. Typically, ZT is taken at the temperature $\sim \frac{1}{2}(T_0 + T_{isl})$. Carnot efficiency corresponds to $ZT \rightarrow \infty$. For refrigeration, it predicts that the lowest achievable temperature, T_{min} , is given by

$$T_{min}/T_0 = 1 - \frac{1}{2}ZT. \quad (2)$$

Eq. (2) is derived¹ by combining linear response terms (the Peltier effect due to the current I , and heat flow due to the temperature difference, $T_0 - T_{isl}$), with a nonlinear I^2 term corresponding to Joule heating. Heat flow out of the island in Fig. 2a, due to a current I passing through element 1, then the island and then element 2, is

$$J(T_{isl}, I) \simeq \Pi_- I - \Theta_+ (T_0 - T_{isl}) - \frac{1}{2}G_+^{-1}I^2, \quad (3)$$

for $\Pi_- = \Pi_2 - \Pi_1$, $\Theta_+ = \Theta_1 + \Theta_2 + \Theta_{ph}$ and $G_+^{-1} = G_1^{-1} + G_2^{-1}$. Here Π_i , G_i and Θ_i are the Peltier coefficient, the electrical and thermal conductances of element i . The steady-state curve, $J = 0$, gives T_{isl} as a quadratic function of I . The parabola’s minimum is T_{min} in Eq. (2) with $ZT = G_+\Pi_-^2/(\Theta_+T)$.

For a point-contact at pinch-off (see Section III), linear-response^{28,32–37} gives $G_1 = (e^2/h)(1/2)$, $\Pi_1 = -(k_B T_0/e)2\ln(2)$, and³⁸ $\Theta_1 = (k_B^2 T_0/h)(\pi^2/6 - 2[\ln(2)]^2)$. Thus $ZT \simeq 1.4$ so

$$\eta = 0.22(1 - T_0/T_{isl}), \quad T_{min} = 0.3T_0. \quad (4)$$

However, Eq. (3) ceases to apply whenever thermoelectric effects are strong enough that the nonlinear terms that were not included in Eq. (3) become relevant. Heuristically, Eq. (3) fails to get the physics *qualitatively* correct for any system where the nonlinear Peltier term²¹, $\tilde{\Pi}I^2$, is larger than the Joule heating term $\frac{1}{2}G_+^{-1}I^2$. The reason being that including $\tilde{\Pi}I^2$ in Eq. (3) then changes the sign of the prefactor on I^2 ; so one must go beyond I^2 to find the steady-state curve’s minimum. Including this $\tilde{\Pi}$ term will then make the refrigerator *better* than if it were neglected. However higher order terms (I^3 or higher) will then also be crucial in determining the lowest temperature the refrigerator can achieve.

This break-down of the nearly-linear theory as $\tilde{\Pi}$ increases is discussed in Section VI for a particular system (a point-contact in parallel with a tunnel-barrier) in which $\tilde{\Pi}$ can be varied; it indeed occurs when $\tilde{\Pi}$ is of order $\frac{1}{2}G_+^{-1}$. Readers familiar with simple ϕ^4 -theory will see this is similar to the para- to ferro-magnetic crossover of a magnet in a B-field upon reducing the temperature³⁹. However, unlike in ϕ^4 -theory, for small barrier transmission (or a point-contact alone), the analysis shows such strong nonlinearities (catastrophe, etc) that the minimum is not captured by a perturbative expansion in I up to any order.

Of course, the above heuristic argument assumes that nonlinearities in the thermoelectric response are significant when the linear thermoelectric response is significant. While in most cases this is true, the S-N tunnel junction is a counter-example; it has no thermoelectric response in the linear regime (so $ZT = 0$), but does have a large nonlinear response which has been used for refrigeration^{13–15}. This is because the electron and holes have the same transmission at zero bias (so there is no thermoelectric response), but nonlinear charging effects enhance the transmission of electrons over those of holes creating an entirely nonlinear thermoelectric effect. It would be interesting to see if such S-N junctions exhibit the type of catastrophes found in this work for point contacts.

III. FULLY NONLINEAR ANALYSIS FOR POINT-CONTACTS

The thermoelectricity literature^{1–3} discusses $J(T_{\text{isl}}, I)$ — as in Eq. (3) above — rather than $J(T_{\text{isl}}, V)$ for voltage drop, V . This is because different thermoelectric devices are arranged in series electrically (see Fig. 2a,b), so I is the same in all of them (unlike voltage drops). Thus it is easier to get response of a series of elements from each element's $J(T_{\text{isl}}, I)$ than from each element's $J(T_{\text{isl}}, V)$. For complicated non-linear responses, the former is straight-forward while the latter is extremely difficult; thus I consider $J(T_{\text{isl}}, I)$.

I take the island to be classical; i.e. big enough for particles entering it to thermalize to a Fermi distribution at temperature T_{isl} before escaping. I also assume quantum charging effects (Coulomb blockade, etc) within the island are negligible, while classical charging effects ensure electro-neutrality (i.e. that the sum of electrical currents into the island is zero). Refs. [40–44] consider cases where there is a quantum dot in place of the classical island. In our case, each point-contact can be treated by a separate Landauer-Büttiker scattering matrix analysis²⁸, see also Refs. [32–37]. I generalize these heat currents to the nonlinear regime⁴⁵, including electrostatic (Hartree-like) interaction effects in a self-consistent and gauge-invariant manner; as Refs. [24–27] did for charge-current, see also^{46,47}. To go beyond the voltage-squared contributions to transport (which Ref. [24] treated in detail), I use a simple model of interactions, which is none the less gauge-invariant and self-consistent. The charge-current, I_i , and heat-current, J_i , into lead i of a given nanostructure are

$$I_i = - \int_{-\infty}^{\infty} \frac{d\epsilon}{h} \sum_j q \mathcal{A}_{ij}(\{\epsilon - qV_k\}) f_j(\epsilon), \quad (5)$$

$$J_i = - \int_{-\infty}^{\infty} \frac{d\epsilon}{h} \sum_j (\epsilon - qV_i) \mathcal{A}_{ij}(\{\epsilon - qV_k\}) f_j(\epsilon), \quad (6)$$

where $f_j(\epsilon) = (1 + \exp[(\epsilon - qV_j)/(k_B T_j)])^{-1}$ is the Fermi function, and q is the charge of the carriers; electrons

with $q = -e$ in point-contact 1 and holes with $q = e$ in point-contact 2. The energy ϵ and all voltages V_k are measured from the same external reference. The transmission function of a particle through the nanostructure from lead j to lead i is $\mathcal{A}_{ij}(\{\epsilon - qV_k\}) = \text{Tr} [\mathbf{1}_i \delta_{ij} - \mathcal{S}_{ij}^\dagger(\{\epsilon - qV_k\}) \mathcal{S}_{ij}(\{\epsilon - qV_k\})]$, where \mathcal{S}_{ij} is the scattering matrix from lead j to lead i , and the trace is over all modes of those leads. Here \mathcal{S}_{ij} must be found *self-consistently*; it depends on the charge distribution in the nanostructure, which in turn depends on \mathcal{S}_{ij} . Writing \mathcal{S}_{ij} as a function only of energy differences, $\{\epsilon - qV_k\}$, makes the gauge-invariance explicit; it satisfies²⁴ $[(d/d\epsilon) + \sum_k (d/d(qV_k))] \mathcal{A}_{ij} = 0$.

Point-contact 1 is a two-lead nanostructure with electron charge-carriers ($q = -e$). The gauge-invariance means one is free to measure all energies ϵ and voltages V_k (including V_g) from the island's chemical potential (the point-contact's M lead). I assume that a proportion $(1 - a)$ of V_L is screened by the electrostatic gates a long way from the narrowest-point of the point-contact, while the rest is screened self-consistently by the electron-gas (Fig. 2d) close to the point-contact. Then the *screened* point-contact induces a potential barrier of height, E_{pc} (measured from the island's chemical potential), typically obeying $E_{\text{pc}} - E_g = E_{\text{scr}}(aqV_L)$, where E_{scr} is due to screening. Here E_g can be tuned at will, since it is eV_g minus a geometry-dependent constant. Assuming a long enough point-contact that there is negligible tunnelling, one has $\mathcal{A}_{\text{LM}}(\epsilon - E_{\text{pc}} > 0) = -1$ (perfect transmission) and $\mathcal{A}_{\text{LM}}(\epsilon - E_{\text{pc}} < 0) = 0$ (no transmission)⁴⁸. As an example, the appendix gives a simple screening model for which I derive $E_{\text{scr}}(aqV_L)$ self-consistently. However, in what follows I allow the nature of screening (both a and the form of $E_{\text{scr}}(aqV_L)$) to be completely arbitrary.

For any given V_L , one can adjust V_g to tune to pinch-off ($E_{\text{pc}} = 0$). If the gates dominate screening ($a \rightarrow 0$), then E_{pc} is V_L -independent, making this straightforward. Otherwise, the point-contact should be calibrated prior to use; finding the pinch-off point (the V_g at which current starts to flow), as a function of V_L . At pinch-off, the currents from point-contact 1 into the island are

$$I(T_{\text{isl}}, V_L) = \frac{ek_B}{h} [T_{\text{isl}} \ln(2) - T_0 \ln(1 + e^{-eV_L/k_B T_0})], \quad (7)$$

$$J_1(T_{\text{isl}}, V_L) = -\frac{k_B^2}{h} \left[T_{\text{isl}}^2 \frac{\pi^2}{12} + T_0^2 \text{Li}_2(-e^{-eV_L/k_B T_0}) \right], \quad (8)$$

where $\text{Li}_2(z)$ is a dilogarithm function. Eqs. (7,8) give

$$J_1(T_{\text{isl}}, I) = -\frac{k_B^2 T_0^2}{h} \left[\frac{\pi^2 T_{\text{isl}}^2}{12 T_0^2} + \text{Li}_2(1 - \exp[\mathcal{J}(T_{\text{isl}}, I)]) \right], \quad (9)$$

where I define $\mathcal{J} = h[I_{\text{max}}(T_{\text{isl}}) - I]/(ek_B T_0)$ and note that $I \leq I_{\text{max}}(T_{\text{isl}}) = ek_B T_{\text{isl}} \ln[2]/h$. This function is given by the color plot in Fig. 1. For point-contact 2 (where carriers are holes not electrons) one takes $-e \leftrightarrow e$, then $J_2(T_{\text{isl}}, I) = J_1(T_{\text{isl}}, I)$ since $I_2 = -I$.

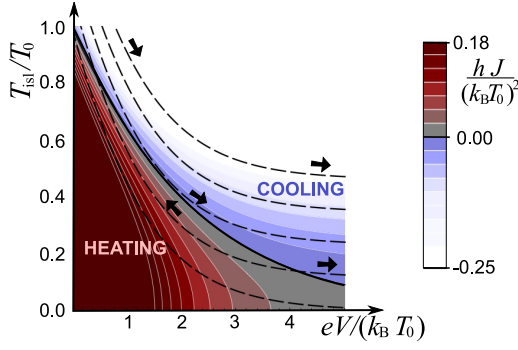


Figure 3: Heat-current as a function of V and T_{isl} , with the steady-state, $J = 0$, marked by the black-curve (note the darkest color is used for all $hJ/(k_B T_0)^2 > 0.18$ and white for all $hJ/(k_B T_0)^2 < -0.25$). Superimpose are lines of constant current (dashed), these are $hI/(ek_B T_0) = 0, 0.08, 0.16, 0.24, 0.32$ from bottom to top.

For $J \ll 1$, one can use $\text{Li}_2(z) = z + \mathcal{O}[z^2]$ to write

$$J_1 = (k_B^2 T_0^2 / h) [J - (\pi^2 / 12) (T_{\text{isl}} / T_0)^2 + \mathcal{O}[J^2]], \quad (10)$$

so J_1 as a quadratic in temperature and linear in current; the reverse of the nearly-linear theory in Eq. (3). This approximation captures the features of the exact result plotted in Fig. 1, except the top-left corner. This corner is the linear-response regime (small $(T_0 - T_{\text{isl}})$ and I), where one has Eq. (9) with $\text{Li}_2(-1 + z) \simeq -\pi^2/12 + \ln[2]z$.

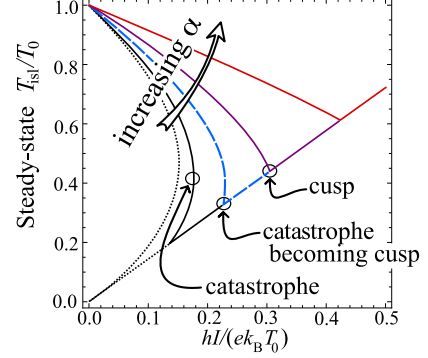
IV. REFRIGERATION WITHOUT PHONONS OR PHOTONS

Heat flow into the island is $J_{\text{total}} \propto J_1$ for the devices in Fig. 2a,b; $J_{\text{total}} = 2J_1$ for the thermocouple. The black curves in Fig. 1 are $J_{\text{total}} = 0$, giving the steady-state temperature (solid for stable steady-states and dashed for unstable ones). Solid curves give the temperature the island will be cooled to by a current I . Eq. (10) tells us the steady-state has I as a quadratic function of T_{isl} ; this approximation gives the catastrophe at $eI_c/(ek_B T_0) = 3(\ln[2]/\pi)^2 \simeq 0.14$ with $T_{\text{isl}}/T_0 = 6\ln[2]/\pi^2 \simeq 0.42$, which is very close to the exact solution in Fig. 1.

A. Voltage dependence of cooling.

As mentioned above, one typically consider the response of thermoelectric devices as a function of current I , rather than voltage V , since I is conserved in series electrical circuits like those in Fig. 2a,b. However the origin of the catastrophe can be seen in Fig. 3, which compares the nonlinear response of the point-contact as a function of voltage, Eq. (8), with curves of constant current given by Eq. (7). Curves with $I < I_c$,

(a) steady-state curves for weak phonon back-flows



(b) steady-state curve for stronger phonon back-flow

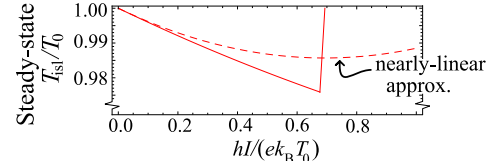


Figure 4: (a) Steady-state refrigeration curves, $J(T_{\text{isl}}, I) = 0$, for increasing heat flow due to phonons and photons; $\alpha/\alpha_0 = 0, 0.02, 0.06, 0.12, 0.3$. (b) The solid v-shaped curve is the steady-state refrigeration curve, $J(T_{\text{isl}}, I) = 0$ for $\alpha = 10\alpha_0$, i.e. about 30 times stronger phonon back-flow than (a)'s upper-most curve. It is very different from the nearly-linear theory for the same α (dashed parabola).

such as $hI/(ek_B T_0) = 0.08$, cross from cooling to heating and back again, while curves with $I > I_c$, such as $hI/(ek_B T_0) = 0.16, 0.24, 0.32$, never enter the heating regime. For larger I , the temperature saturates at a higher value. All of this fits with Fig. 1.

Note that if one wants the voltage response of the circuits in Fig. 2a,b one cannot easily get it from the voltage response of each element, as plotted in Fig. 3. This is because the voltage drop across each thermoelectric element depends nonlinearly on T_{isl} , even when the total voltage drop across all elements is fixed (unless all thermoelectric elements have the same $I(T_{\text{isl}}, V)$). Indeed the simplest way to get the voltage response of the circuits in Fig. 2a,b is to take the heat-flow in each circuit element as a function of I (as plotted in Fig. 1). Since I is the same in every element, one can get the heat-flow as a function of the voltage drop across the circuit as the sum of voltage drops across each element (as a function of T_{isl} and I).

V. REFRIGERATION WITH PHONONS OR PHOTONS

I assume the metallic island is a suspended nanostructure²⁹ in a cryostat at 0.3K, coupled to the substrate by suspended nanowires carrying the wires forming the cooling circuit. Wien's displacement law gives a photon wavelength of 10mm at 0.3K. For any island smaller than a few millimetre, bulk blackbody radiation

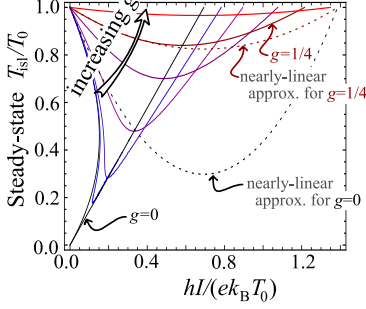
Refrigeration with point-contact *in parallel* with a tunnel-barrier

Figure 5: Steady-state refrigeration curves for a composite system; point-contact in parallel with a barrier of conductance $G_{\text{barrier}} = e^2 g/h$ for $g = 0, 0.001, 0.005, 0.025, 0.1, 0.25, 1$ (solid curves). The parabolas (dashed) are the nearly-linear approximation for $g = 0, 1/4$; for $g = 1$ the difference from the exact curve is not visible.

is replaced by a single photon mode of noise-flow between the island and its environment along the wires^{49,50}, with $J_{\text{ph}} = r\alpha_0(T_0^2 - T_{\text{isl}}^2)$, where $\alpha_0 = \pi^2 k_B^2/(6h)$ is the “quantum” of heat-flow and r is the mode’s transmission. If the environment part of the circuit has an inductance⁵¹ $> 1\mu\text{H}$ (or its capacitor equivalent), then $r \ll 1$.

For a nanowire with N_{ph} phonon (vibrational) modes, $J_{\text{ph}} = \alpha(T_0^2 - T_{\text{isl}}^2)$, with $\alpha = N_{\text{ph}}\mathcal{T}\alpha_0$, with average transmission per mode of \mathcal{T} . Experimental nanowires²⁹ show $\alpha \sim 0.3\alpha_0$ at ambient temperature $T_0 = 0.3\text{K}$. For this α , the steady-state curve has a pronounced cusp (uppermost v-shaped curve in Fig. 4a), very different from the parabola given by the standard nearly-linear theory. Fig. 4b shows that this cusp persists up to such larger α that there is very little refrigeration (note the vertical axis shows T_{isl}/T_0 is only slightly below one for any I). The α chosen for the plot in Fig. 4b corresponds to that observed in experiments in Ref. [29,30] at 3K. This is about thirty times larger than the minimum phonon conductance observed in Ref. [29] at 0.3K. It also shows that the nearly-linear theory (dashed parabola) significantly under-estimates the optimum refrigeration.

Taking the longitudinal phonon modes (velocity 9000ms^{-1}) and three types of transverse modes (velocity 6000ms^{-1}), the above experimental nanowires³⁰ (with cross-section $200\text{nm} \times 100\text{nm}$) have $N_{\text{ph}} \sim 20$ at $T_0 \sim 0.3\text{K}$. Evidently $\mathcal{T} \sim 1/60$, its smallness is probably due to the frequency mis-match between the phonons in the nanowire and the bulk. If wires with cross-section $50\text{nm} \times 50\text{nm}$ could be made, then $N_{\text{ph}} \sim 4$. Thus $\alpha \sim 0.06\alpha_0$ can be expected (i.e. five times smaller than the current nanowires), the dashed curve in Fig. 4a show the catastrophe emerging at such α . To reduce α further, one can add surface roughness or serpentines³⁰.

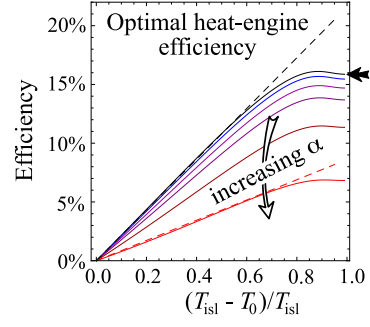


Figure 6: Heat-engine efficiency curves for $\alpha/\alpha_0 = 0, 0.02, 0.06, 0.12, 0.3, 1$. Dashed lines are the linear-response predictions, Eq. (1), for $\alpha/\alpha_0 = 0, 1$.

VI. CROSS-OVER FOR POINT-CONTACT IN PARALLEL WITH BARRIER

I ask how one can induce a transition to the parabolic behavior in Eq. (3), since phonons, etc, do not do so? I find that a transition only occurs upon reducing the ϵ -dependence of \mathcal{A}_{ij} , lowering the ratio of the thermoelectric response to the usual electric response — for example, replacing the point-contact with a composite system consisting of a point-contact in *parallel* with a tunnel-barrier whose transmission is ϵ -independent. Fig. 5 shows the steady-state response of the composite system, for barrier conductance $G_{\text{barrier}} = e^2 g/h$. Upon increasing g from zero, a transition occurs at $g = g_c \sim 1/200$; for $g > g_c$, the curve is single-valued, so T_{min} becomes a continuous function of I . The nearly-linear theory works for $g \gtrsim 1$, deviations are still visible for $g = 1/4$ (cf. solid and dashed curves). This fits the argument in Section II, since the composite system has $\tilde{\Pi} < \frac{1}{2}G^{-1}$ for $g > (3 \ln[2] - 1)/2 \simeq 0.53$.

VII. HEAT-ENGINE EFFICIENCY

Returning to the case of a point-contact alone (without a tunnel-barrier), I now consider its maximum efficiency as a heat engine. For $T_{\text{isl}} > T_0$, the circuit in Fig. 2a provides electrical power $P = IV$ to any load connected between L and R. To calculate the maximum electrical power $P(T_{\text{isl}}, I)$ that a heat engine can extract from a heat flow $J(T_{\text{isl}}, I)$, one assumes a Ohmic load — so $V(T_{\text{isl}}, I) = I/G_{\text{load}}$ — is connected across its terminals, and adjust G_{load} to optimize the ratio of the power at the load $P(T_{\text{isl}}, I) = IV(T_{\text{isl}}, I)$ to the heat flow $J(T_{\text{isl}}, I)$. This corresponds to finding the $I = I_{\text{opt}}$ which maximizes $P(T_{\text{isl}}, I)/J(T_{\text{isl}}, I)$. Maxima and minima are given by $P'J = PJ'$ where the primed is (d/dI). Given $V(T_{\text{isl}}, I)$ and $J(T_{\text{isl}}, I)$, one can solve this to find I_{opt} . Optimal efficiency is $\eta = P(I_{\text{opt}})/J(I_{\text{opt}})$.

As a warm-up, I consider the usual linear problem, with $V(T_{\text{isl}}, I) = S(T_{\text{isl}} - T_0) - G^{-1}I$ and $J(T_{\text{isl}}, I) = \Theta(T_{\text{isl}} - T_0) + \Pi I$, with $\Pi = \Gamma/G$ and $S = B/G$. Calcu-

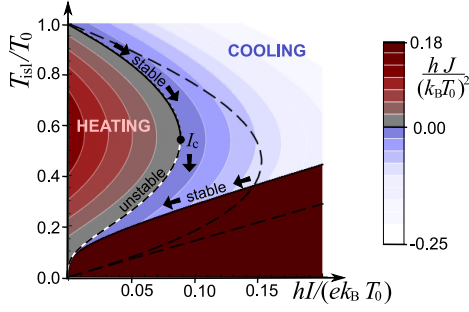


Figure 7: The heat-current when the barrier peak is at $E_{pc} = k_B T_0/4$. The results which give this curve will be discussed elsewhere. For comparison, the thin-dashed curves are the steady-state for $E_{pc} = 0$ in Fig. 1.

late the optimal efficiency in the manner described above, I find $I_{opt} = (\Theta/\Pi)[\sqrt{Z(T_{isl})T_{isl}} + 1 - 1](T_{isl} - T_0)$. Dropping T -dependences of ZT , one gets Eq. (1).

Now I use the same method to get the efficiency in the nonlinear regime. An analytic solution of $P'J = PJ'$ can be found for large (T_{isl}/T_0) , using the fact (confirmed by the numerics) that in this limit $-eV_1(I_{opt})/(k_B T_0) \gg 1$ with $V_1 < 0$. Otherwise the solution must be found numerically (see below). For large (T_{isl}/T_0) , I take $\ln[1 + e^\mu] \rightarrow \mu$ and $\text{Li}_2(-e^\mu) \rightarrow -\frac{1}{2}\mu^2$ for large μ , and find $eV_1(T_{isl}, I)/(k_B T_0) \simeq -t_{isl} \ln[2] + \tilde{I}$ with $hJ_1(T_{isl}, I)/(k_B T_0)^2 \simeq -\kappa t_{isl}^2/2 - \ln[2] \tilde{I} t_{isl} + \tilde{I}^2/2$, where I define $t_{isl} = T_{isl}/T_0$, $\tilde{I} = hI/(ek_B T_0)$ and $\kappa = \pi^2/6 - \ln^2[2] \simeq 1.16$. The heat-current from the hot source into the device is $J(T_{isl}, I) = -J_1(T_{isl}, I)$, and $P = -V_1(T_{isl}, I)I$ (given that $V_1 < 0$). In this case $P'(T_{isl}, I_{opt})J(T_{isl}, I_{opt}) = P(T_{isl}, I_{opt})J'(T_{isl}, I_{opt})$ is a quadratic equation for I_{opt} ; solving it gives

$$\frac{hI_{opt}}{ek_B T_0} = \frac{\kappa}{\ln[2]} \left[\sqrt{1 + \ln^2[2]/\kappa} - 1 \right] \frac{T_{isl}}{T_0},$$

Without phonons or photons, the optimal efficiency tends to $1 - \sqrt{1 - 6(\ln[2]/\pi)^2} \simeq 15.9\%$ for $T_{isl} \rightarrow \infty$ (solid arrow in Fig. 6). Solving $P'J = PJ'$ with Eqs. (7,9) numerically, to find I_{opt} for different T_{isl}/T_0 , I plot η against $(T_{isl} - T_0)/T_{isl}$ in Fig. 6. I have no simple argument why the curves are slightly peaked at $(T_{isl} - T_0)/T_{isl} \sim 0.85$.

VIII. CATASTROPHE AWAY FROM PINCH-OFF

Fig. 7 gives an example showing the catastrophe is still present when the point-contact is away from pinch-off; i.e. when the barrier's peak is above the chemical potential of the island in Fig. 1. The catastrophe is present when $0 < E_{pc} \lesssim k_B T_0$, which corresponds to the parameter regime where a significant thermoelectric response was found experimentally in Ref. [18]. The formulas leading to Fig. 7 are similar to Eqs. (7-9) but rather longer, so I do not give them here.

IX. CONCLUDING REMARKS

I have shown that the point-contact (arguably the simplest thermoelectric nanostructure) has a rich nonlinear behavior. In particular when it is used as a refrigerator, it exhibits multiple steady-states (stable and unstable) and a fold catastrophe; or a sharp-cusp when there is significant phonon back-flow. I see no reason to think that more complicated nanoscale thermoelectric systems⁴⁻¹¹ have less rich behaviors. Indeed a large ZT is a strong hint that its nonlinear Peltier term, $\tilde{\Pi}I^2$ may dominate over its Joule heating term $-\frac{1}{2}G^{-1}I^2$. Section II then gives a simple argument that ZT ceases to give even a qualitative indication of how good a refrigerator it is. Thus the fully nonlinear response of such systems require detailed study, beyond the weak nonlinearities considered in Refs. [17,21,52,53].

Finally, I recall that this work considered the case where the charging effects of electrons at the point contact were well screened by the gates (or could be compensated for by the gates), meaning the E_{pc} in Fig. 2 does not significantly change with bias. Elsewhere, I will show that qualitatively similar effects can occur for point-contacts (and other systems) without gates, for which E_{pc} depends on the bias.

Since the submission of this work, a number of closely related works have appeared⁵²⁻⁵⁷.

A. Acknowledgements

I thank F. Hekking, G. Rastelli, C. Stafford, and particularly Ph. Jacquod, for insightful comments at various stages of this work.

Appendix A: Example of a self-consistent solution

Here is a simple model of the point-contact for which the self-consistent solution can be found easily. However, the results in the body of the manuscript apply for almost any self-consistent model. The point-contact is treated as a one-dimensional scattering problem (along the x-axis), see Fig. 2d. Close to the point-contact, this takes the form $qV(x) = E_g - \kappa x^2 + qV_{scr}(x - x_{pc})$ with energy measured from the island's chemical potential. The transverse confinement induces the $(E_g - \kappa x^2)$ -term, where E_g can be tuned, since it equals eV_g minus a geometry-dependent constant. The qV_{scr} -term is screening inside the electron gas, which I take as

$$V_{scr}(x) = \begin{cases} aV_L & \text{for } x < -l_{scr} \\ aV_L(l_{scr} - x)/(2l_{scr}) & \text{for } |x| \leq l_{scr} \\ 0 & \text{for } x > l_{scr} \end{cases}$$

with x_{pc} being the self-consistently determined peak of $qV(x)$. A little algebra gives $x_{pc} = -aqV_L/(4\kappa l_{scr})$, thus the energy at the peak is $E_{pc} = qV(x_{pc}) = E_g +$

$\frac{1}{2}aqV_L(1 - aqV_L/(8\kappa l_{\text{scr}}^2))$. Finally I note that both a and l_{scr} depend on the scattering matrix of the junction, which in turn depends on E_{pc} . To solve this problem self-consistently, I assume one is in the regime where $e_{\text{pc}} = E_{\text{pc}} - E_g$ is small enough to approximate $a = a_0(1 + b_a e_{\text{pc}})$ and $l_{\text{scr}} = l_{\text{scr}0}(1 + b_l e_{\text{pc}})$. If necessary, $a_0, l_{\text{scr}0}, b_a, b_l$ can be found by simulating Poisson's equation; typically e_{pc} is small for small a . Then E_{pc} is equal to a linear function of itself; re-arranging this gives

$$E_{\text{pc}} - E_g = \frac{a_0 q V_L / 2 - C(q V_L)}{1 - a_0 b_a q V_L + 2C(q V_L) [b_a - b_l]},$$

where I define $C(q V_L) = (a_0 q V_L / l_{\text{scr}0})^2 / (16\kappa)$. Thus the right hand side of this equation is the $E_{\text{scr}}(aq V_L)$ men-

tioned in the body of the text. As mentioned earlier, I assume that tunnelling at energies $\epsilon < E_{\text{pc}}$ is negligible, so $\mathcal{A}_{\text{LM}}(\epsilon - E_{\text{pc}} > 0) = -1$ and $\mathcal{A}_{\text{LM}}(\epsilon - E_{\text{pc}} < 0) = 0$. To see that this respects gauge-invariance, I recall that $\epsilon, E_{\text{pc}}, V_{L,g}$ are all measured relative to the island's potential, and replace them by quantities measured from a fixed external reference, so the island is at \tilde{V}_M . For clarity, here (unlike in the paragraph containing Eq. (6)) it is necessary to use a tilde to explicitly indicate quantities measured from the external reference. I make the replacement $q V_L = (\tilde{\epsilon} - q \tilde{V}_M) - (\tilde{\epsilon} - q \tilde{V}_L)$. From this, one sees that $\mathcal{A}_{\text{LM}}(\epsilon - E_{\text{pc}})$ is only a function of the set of differences $\{\tilde{\epsilon} - q \tilde{V}_k\}$, and so respects gauge-invariance.

-
- ¹ H.J. Goldsmid, *Thermoelectric Refrigeration* (Temple Press, London, 1964), chapt 1. H.J. Goldsmid, *Introduction to Thermoelectricity* (Springer, Heidelberg, 2009), chapt 2.
 - ² F.J. DiSalvo, Science **285**, 703 (1999).
 - ³ A. Shakouri and M. Zebarjadi Chapt 9 of *Thermal nanosystems and nanomaterials*, S. Volz (Ed.) (Springer, Heidelberg, 2009). A. Shakouri, Annu. Rev. Mater. Res. **41**, 399 (2011).
 - ⁴ G. Casati, C. Mejía-Monasterio, and T. Prosen, Phys. Rev. Lett. **101**, 016601 (2008).
 - ⁵ D. Nozaki, H. Sevingli, W. Li, R. Gutiérrez, and G. Cuniberti, Phys. Rev. B **81**, 235406 (2010).
 - ⁶ K.K. Saha, T. Markussen, K.S. Thygesen, and B.K. Nikolić, Phys. Rev. B **84**, 041412(R) (2011).
 - ⁷ M. Wierzbicki and R. Swirkowicz, Phys. Rev. B **84**, 075410 (2011).
 - ⁸ O. Karlström, H. Linke, G. Karlström, and A. Wacker, Phys. Rev. B **84**, 113415 (2011).
 - ⁹ T. Gunst, T. Markussen, A.-P. Jauho, and M. Brandbyge, Phys. Rev. B **84**, 155449 (2011).
 - ¹⁰ G. Rajput, and K.C. Sharma, J. Appl. Phys. **110**, 113723 (2011).
 - ¹¹ P. Trocha and J. Barnaś, Phys. Rev. B **85**, 085408 (2012).
 - ¹² F. Giazotto, T.T. Heikkilä, A. Luukanen, A.M. Savin, J.P. Pekola, Rev. Mod. Phys. **78**, 217 (2006). J.T. Muhonen, M. Meschke, J.P. Pekola, Rep. Prog. Phys. **75**, 046501 (2012).
 - ¹³ M.M. Leivo, J.P. Pekola and D.V. Averin, Appl. Phys. Lett. **68**, 1996 (1996).
 - ¹⁴ A.M. Clark, N.A. Miller, A. Williams, S.T. Ruggiero, G.C. Hilton, L.R. Vale, J.A. Beall, K.D. Irwin, and J. N. Ullom, Appl. Phys. Lett. **86**, 173508 (2005).
 - ¹⁵ S. Rajauria, P.S. Luo, T. Fournier, F.W.J. Hekking, H. Courtois, and B. Pannetier, Phys. Rev. Lett. **99**, 047004 (2007). S. Rajauria, P. Gandit, F.W.J. Hekking, B. Pannetier, H. Courtois, J. Low Temp. Phys. **154** 211 (2009).
 - ¹⁶ For bulk semiconductors, linear response (Boltzmann) transport theory works when the temperature difference on the scale of the inelastic scattering length is small compared with the average temperature at that point. The inelastic scattering length (typically 1-100nm at 290K) is very much less than the length over which temperature drops (length of semiconductor, e.g. millimetres). Then a linear theory works well even when the temperature drop is large, although nonlinear corrections have been studied¹⁷. In contrast, nanostructures are often smaller than the inelastic scattering length (often much more than 1μm at 1K). Ideally the whole temperature drop occurs across this nanostructure, making linear-response theory inappropriate when the temperature drop is significant.
 - ¹⁷ M. Zebarjadi, K. Esfarjani, and A. Shakouri, Appl. Phys. Lett. **91**, 122104 (2007); in *Thermoelectric Power Generation* by T.P. Hogan, J. Yang, R. Funahashi, T. Tritt (Eds.), MRS Symposia Proceedings No. **1044**, (Materials Research Society, Pittsburgh, 2008) p. U10.
 - ¹⁸ L.W. Molenkamp, Th. Gravier, H. van Houten, O.J.A. Buijk, M.A.A. Mabesoone, and C.T. Foxon, Phys. Rev. Lett. **68**, 3765 (1992). H. van Houten, L.W. Molenkamp, C.W.J. Beenakker, and C.T. Foxon, Semicond. Sci. Technol. **7**, B215 (1992).
 - ¹⁹ U. Ghoshal, S. Ghoshal, C. McDowell, L. Shi, S. Cordes, and M. Farinelli, Appl. Phys. Lett. **80**, 3006 (2002).
 - ²⁰ E.N. Bogachek, A.G. Scherbakov and U. Landman, Solid State Comm. **108**, 851 (1998). This work calculates the non-linear differential Peltier coefficient $\Pi_{\text{diff}} = dJ/dI$, even though some formulas assume linear behavior.
 - ²¹ M.A. Çipiloğlu, S. Turgut and M. Tomak, Phys. Stat. Sol. (b) **241**, 2575 (2004).
 - ²² N. Nakpathomkun, H.Q. Xu, and H. Linke, Phys. Rev. B **82** 235428 (2010).
 - ²³ M. Moskalets, JETP Lett. **62**, 719 (1995).
 - ²⁴ T. Christen and M. Büttiker, Europhys. Lett. **35**, 523 (1996).
 - ²⁵ D. Sanchez and M. Buttiker, Phys. Rev. Lett. **93**, 106802 (2004).
 - ²⁶ J. Meair and Ph. Jacquod, J. Phys.: Condens. Matter **24**, 272201 (2012).
 - ²⁷ D. Sánchez, and R. López, Phys. Rev. Lett. **110**, 026804 (2013).
 - ²⁸ P.N. Butcher, J. Phys.: Condens. Matter, **2**, 4869 (1990).
 - ²⁹ J.S. Heron, T. Fournier, N. Mingo, O. Bourgeois, Nano Lett. **9**, 1861 (2009).
 - ³⁰ J.-S. Heron, C. Bera, T. Fournier, N. Mingo, and O. Bourgeois, Phys. Rev. B **82**, 155458 (2010).
 - ³¹ S. Gasparinetti, F. Deon, G. Biasiol, L. Sorba, F. Beltram, and F. Giazotto, Phys. Rev. B **83**, 201306(R) (2011).

- ³² H.-L. Engquist and P.W. Anderson, Phys. Rev. B **24**, 1151 (1981).
- ³³ U. Sivan and Y. Imry, Phys. Rev. B **33**, 551 (1986).
- ³⁴ N.R. Claughton and C.J. Lambert, Phys. Rev. B **53**, 6605 (1996).
- ³⁵ Ph. Jacquod and R.S. Whitney, Europhys. Lett. **91**, 67009 (2010).
- ³⁶ Y.-S. Liu, B.C. Hsu, and Y.C. Chen, J. Phys. Chem. C **115**, 6111 (2011).
- ³⁷ Ph. Jacquod, R.S. Whitney, J. Meair, and M. Büttiker, Phys. Rev. B **86**, 155118 (2012).
- ³⁸ Θ_i is the thermal conductance for $I = 0$ (not $V = 0$).
- ³⁹ In ϕ^4 -theory at high temperatures, the ϕ^2 -term is positive and determines the minimum of free-energy. At low temperatures, the ϕ^2 term is negative and the minimum is determined by a higher order term (the ϕ^4 -term). In the refrigerator, the role of ϕ is played by I , while the parameter which controls the sign of the quadratic term is $\tilde{\Pi}$ rather than temperature.
- ⁴⁰ O. Entin-Wohlman, Y. Imry, and A. Aharony, Phys. Rev. B **82**, 115314 (2010).
- ⁴¹ B. Sothmann, R. Sánchez, A.N. Jordan, and M. Büttiker, Phys. Rev. B **85**, 205301 (2012).
- ⁴² B. Sothmann, and M. Büttiker, EPL **99**, 27001 (2012).
- ⁴³ R. Sánchez and M. Büttiker, EPL **100**, 47008 (2012).
- ⁴⁴ J.-H. Jiang, O. Entin-Wohlman, Y. Imry, New J. Phys. **15**, 075021 (2013). O. Entin-Wohlman, A. Aharony, Y. Imry, arXiv:1306.1813.
- ⁴⁵ R.S. Whitney, Phys. Rev. B **87**, 115404 (2013).
- ⁴⁶ M. Büttiker, J. Phys. Condens. Matter, **5**, 9361 (1993). M. Büttiker, A. Prêtre, and H. Thomas, Phys. Rev. Lett. **70**, 4114 (1993); Z. Phys. B, **94**, 133 (1994). T. Christen and M. Büttiker, Phys. Rev. Lett. **77**, 143 (1996).
- ⁴⁷ C. Petitjean, D. Waltner, J. Kuipers, I. Adagideli, K. Richter, Phys. Rev. B, **80**, 115310 (2009).
- ⁴⁸ The results are unchanged if a little bit of tunnelling means that $\mathcal{A}_{LM}(\epsilon)$ goes smoothly from 0 to -1 on a scale less than $k_B T_{isl}$.
- ⁴⁹ J.B. Pendry, J. Phys. A:Math. Gen. **16**, 2161 (1983).
- ⁵⁰ D.R. Schmidt, R.J. Schoelkopf, and A.N. Cleland, Phys. Rev. Lett. **93**, 045901 (2004).
- ⁵¹ L.M.A. Pascal, H. Courtois, and F.W.J. Hekking, Phys. Rev. B **83**, 125113 (2011).
- ⁵² J. Meair, and Ph. Jacquod, J. Phys.: Condens. Matter, **25**, 082201 (2013).
- ⁵³ R. López, and D. Sánchez, Phys. Rev. B **88**, 045129 (2013).
- ⁵⁴ A.N. Jordan, B. Sothmann, R. Sánchez, and M. Büttiker, Phys. Rev. B **87**, 075312 (2013).
- ⁵⁵ S.-Y. Hwang, D. Sánchez, M. Lee, and R. López, arXiv:1306.6558.
- ⁵⁶ R.S. Whitney, arXiv:1306.0826.
- ⁵⁷ S. Hershfield, K.A. Muttalib, B.J. Nartowt, arXiv:1307.5670.